REPORT 1074

HYDRODYNAMIC IMPACT OF A SYSTEM WITH A SINGLE ELASTIC MODE I—THEORY AND GENERALIZED SOLUTION WITH AN APPLICATION TO AN ELASTIC AIRFRAME [1]

By Wilbur L. Mayo

SUMMARY

Solutions of impact of a rigid prismatic float connected by a massless spring to a rigid upper mass are presented. The solutions are based on hydrodynamic theory which has been experimentally confirmed for a rigid structure.

Equations are given for defining the spring constant and the ratio of the sprung mass to the lower mass so that the two-mass system provides representation of the fundamental mode of an airplane wing. The forces calculated are more accurate than the forces which would be predicted for a rigid airframe since the effect of the fundamental mode on the hydrodynamic force is taken into account. The response of the two-mass system gives the response of the represented mode and, although no provision is made for taking into account the effect of secondary modes on the hydrodynamic force, means are indicated whereby the results may be used to approximate the response of modes other than the fundamental mode.

Time histories of the hydrodynamic force and structural response are given for wide ranges of mass distribution and ratio of natural period to the period of the impact. By use of nondimensional coefficients these results are made applicable to different combinations of velocity, weight, angle of dead rise, and fluid density. Although the equations permit solutions for different combinations of flight-path angle and trim, an approximation is given for correcting the results for the combination for which solutions are given to other conditions within a narrow range indicated to be of primary interest to the design engineer.

In a comparison of the theoretical data with data for a severe flight-test landing impact, the effect of the fundamental mode on the hydrodynamic force is considered and response data are compared with experimental data. Consideration of the fundamental mode alone fails to account for the fact that during the impact partial failure of the inboard-engine mounts occurred, but use of the theoretical solutions to approximate the effects of further wing torsion leads to substantial agreement.

INTRODUCTION

In recent years the development of large airplanes has caused the elastic behavior of airframe structures during landing impact to become important. The work which has been done on this problem has been handicapped by lack of proper knowledge of the time history of applied ground reaction. This situation has been particularly acute for seaplanes because of difficulties in measuring the hydrodynamic force, the seaway, and the manner of contact with the seaway.

In order to facilitate the interpretation of flight data and to lead to the prediction of design loads on a rational basis, a theoretical hydrodynamic study was made and tests of a rigid float were conducted at the Langley impact basin. Since the results of these tests agree with the theoretical results for wide ranges of the pertinent variables in numerous force time histories (reference 1), it is assumed that the theory may also be used in considering the effect of the upper-structure elasticity of a seaplane on the motion and force characteristics of the hull proper, which is assumed to be rigid.

The bending of wings during impact, which for modern flying boats is the primary structural action, is considered in the present report by reducing the fundamental mode to an equivalent two-mass system. The results are presented in a form suited to general application and are compared with experimental results for a particular case. The equations showing the method of solution are included in appendix A, and a sample data sheet is given as table I.

SYMBOLS

t_n	time required for one-fourth cycle of natural vibration
t_i	time between initial contact and maximum hydrodynamic force for rigid structure
t	time elapsed after initial contact
m_L	lower, or hull, mass of two-mass system
m_S	upper, or sprung, mass of two-mass system
m	gross mass (W/g or m_S+m_L)
W	gross weight
g	acceleration due to gravity
K	spring constant of spring connecting m_S and m_L, force per unit deflection
n_i	acceleration normal to water surface of nodal point of elastic system, multiples of acceleration of gravity; for two-mass system, acceleration of center of gravity
n_o	oscillatory acceleration of hull about center of gravity of two-mass system or nodal point of represented mode, multiples of the acceleration of gravity

[1] Supersedes NACA TN 1398, "Solutions for Hydrodynamic Impact Force and Response of a Two-Mass System with an Application to an Elastic Airframe" by Wilbur L. Mayo, 1947.

V_0 resultant velocity at instant of contact with water surface

ρ mass density of fluid

τ angle of trim; angle of hull keel with respect to plane of water surface

γ_0 flight-path angle at contact; angle between flight path and plane of water surface

β angle of dead rise

C_t nondimensional time coefficient $\left(tV_0\left(\frac{\rho g}{W}\right)^{1/3}\right)$

C_l nondimensional load-factor coefficient $\left(\frac{n_z}{V_0^2}\left(\frac{g^2W}{\rho}\right)^{1/3}\right)$

C_d nondimensional draft coefficient $\left(y_{a_{max}}\left(\frac{\rho g}{W}\right)^{1/3}\right)$

$y_{a_{max}}$ draft at instant of maximum acceleration

f_n natural bending frequency

Where units are not given, any consistent system of units may be used.

THEORY

HYDRODYNAMIC

The hydrodynamic theory used in the present report is the same as that developed in references 1 and 2. A basic differential equation which gives the instantaneous force in terms of the instantaneous position and motion of the float is given in reference 2. This equation is used herein to determine the effect of airframe elasticity in altering the motion and force time history (appendix A). The solution is based on the assumption that the float does not change trim during impact. In this connection the pitching moment may be large, but the time of the impact is short enough to warrant (at the present stage) neglect of the resulting angular velocities and displacements.

The solution presented herein is for a prismatic float with such beam loading that the chines do not immerse during impact. For waves that give the severe design condition of full-length impact, conventional beam loadings are small enough to cause the maximum force to occur at drafts sufficiently small to make the effects of finite width and chine flare secondary. Reference 1 indicates that for a conventional float neglect of the pulled-up bow is justified when the trim is 3° or greater. Although for high-trim landings initial contact by the afterbody may substantially change the trim before the main forebody impact, the neglect of afterbody loads is justified because, during the main impact, the shielding of the afterbody by the forebody due to depth of the step and to keel angle is such as to minimize the importance of afterbody loads.

STRUCTURAL

A simplified representation of primary elasticity of an airframe is shown in figure 1. A rigid lower mass m_L is considered to be connected by a massless spring to a rigid upper mass m_S. In determining the fundamental bending of airplane wings part of the wing mass must be included in m_L and part of the wing lift should be applied to m_L. In the present report the gravity force on each mass is assumed to be balanced by wing lift.

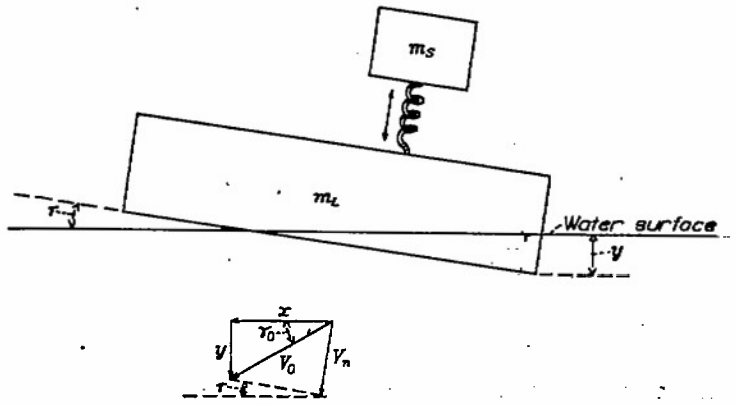

FIGURE 1.—Simplified representation of primary elasticity of an airframe.

The problem of determining the properties of the two-mass system so that it is representative of the primary elastic action of the airplane is rather simple if it is assumed that during the impact the structure deflects with the shape of its fundamental mode of vibration. The requirements are:

(1) The total mass of the simplified system must equal the total mass of the airplane in order that the proper nodal or center-of-gravity accelerations can be obtained.

(2) The energy of vibration for the same amplitude of the hull and lower mass (relative to the nodal point) must be the same for the two-mass system as for the considered mode of the airplane structure.

(3) The natural frequency of the two-mass system must be the same as the frequency of the considered mode of airplane vibration.

Equations which permit determination of the masses and spring constant of the simplified system so that it meets these requirements are given in appendix B. These equations and the foregoing requirements are applicable for both landplanes and seaplanes.

In the present report the represented structural mode is considered to be devoid of vibration prior to the instant of impact. Thus, the computations may represent either a first impact or a subsequent impact resulting from a bounce sufficiently high to cause aerodynamic and structural damping to stop the vibration during the time the seaplane is in the air. This report does not give a representation of successive impacts, such as might occur in seaway, which lead to accumulative or resonant effects. Available flight data indicate that a single heavy impact, such as that considered herein, is the primary cause of structural failures.

The response of the two-mass system is obtained in connection with the calculation of the time history of the hydrodynamic force, and from this result the complete response of the represented mode can be obtained by the simple procedure given in appendix B and demonstrated in the section entitled "Comparison with Experiment." The response of other modes to the force computed on the basis of the fundamental mode can be separately determined and superposed (reference 3). In order to minimize the complexity of the solution, however, the present investigation does not provide for taking into account the effect of the other modes on the hydrodynamic force. Although the other modes may have a substantial effect on the local loads in the structure, the effect of these modes on the

hydrodynamic force is considered to be secondary as compared with the effect of the fundamental mode.

If a large number of solutions for the two-mass system have been made in order to determine the effect of the fundamental mode of different wings on the hydrodynamic force, the response of modes other than the fundamental can be approximated from the use of a solution for a mass ratio and ratio of the time period of the impact force to the natural period of the two-mass system representative of the considered mode. An example of such use to approximate the effects of wing torsion is given in the present investigation in a comparison of results of computations with experimental results.

If the response of more than one mode is considered, the structural and aerodynamic damping, which are not considered herein, are important factors in determining the extent to which the maximum response of the different modes should be superposed without regard to phase relationship. It is expected that the effect of the damping will be most important for the higher modes and that a result leading to conservative design will be obtained if damping is not considered and the maximums of the first two or three modes are superposed without regard to phase relationship.

RESULTS

Solutions of the equations in appendix A were made for wide ranges of the pertinent variables. Time histories of the calculated nodal acceleration, or hydrodynamic force in terms of the weight, are given in figures 2, 3, 4, and 5 for ratios of the sprung mass to the lower mass equal to 0.25, 0.60, 1.00, and 1.36, respectively. Each figure is three-dimensional; the third dimension is t_n/t_t which is a ratio of the period of natural vibration to the speed of the impact. In representing the period of natural vibration, t_n is taken as the time required for one-fourth of a cycle. The speed of the impact is represented by making t_t equal to the time between initial contact and maximum acceleration for a rigid structure. If the time to reach maximum force for the elastic structure should be used in defining t_t, discontinuities in the time to reach maximum force would cause discontinuities in the time-ratio scales of the plots. (See figs. 2 to 5.)

An expression for t_n may be obtained from the relation $t_n=\frac{1}{4}f_n$ and equation (A4) in appendix A. The equation for t_t is as follows:

$$t_t=\frac{C_{t_{a_{max}}}}{V_0}\left(\frac{W}{\rho g}\right)^{1/3} \tag{1}$$

where

$C_{t_{a_{max}}}$ time coefficient at instant of maximum acceleration for rigid body (0.678 for $\beta=22.5°$, $\gamma_0=14°$, and $\tau=3°$)

The expressions for t_n and t_t may be used to determine that

$$\frac{t_n}{t_t}=\frac{\pi V_0}{2C_{t_{a_{max}}}}\left(\frac{m_S m_L}{K}\right)^{1/2}\rho^{1/3}m^{-5/6} \tag{2}$$

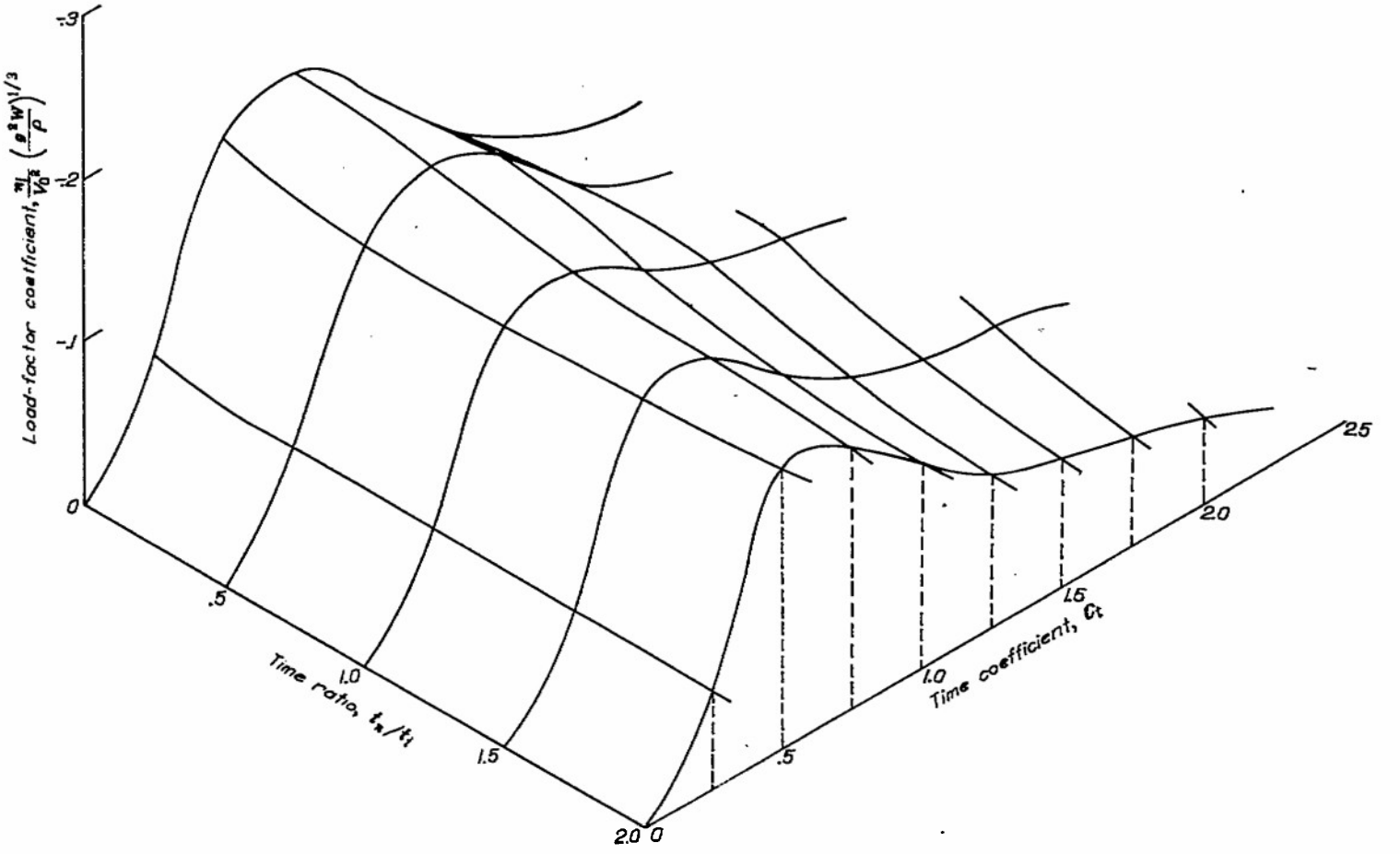

FIGURE 2.—Variation of force time history with time ratio. $\frac{m_S}{m_L}=0.25$; $\beta=22\frac{1}{2}°$; $\gamma_0=14°$; $\tau=3°$.

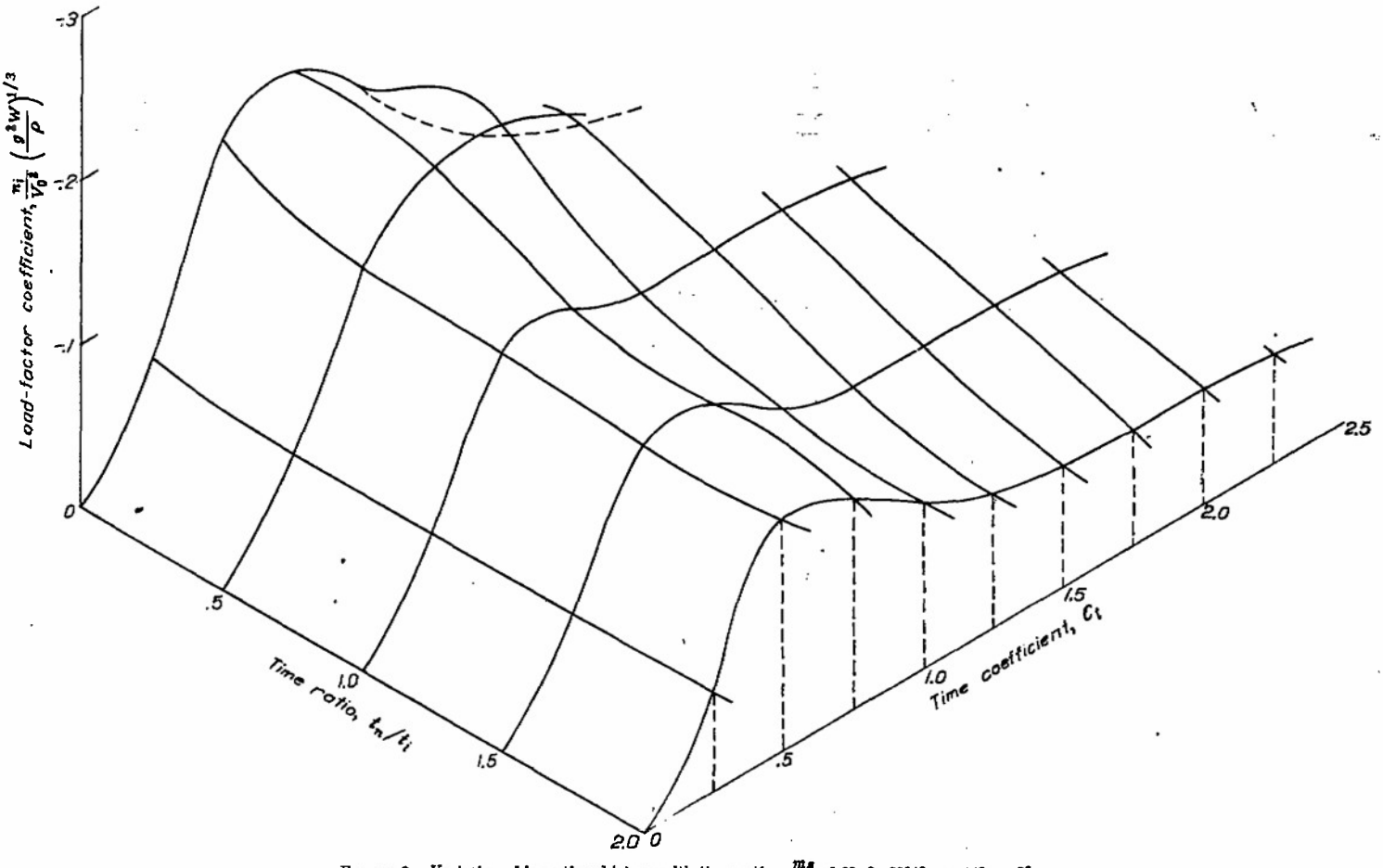

FIGURE 3.—Variation of force time history with time ratio. $\frac{m_s}{m_L}$=0.60; β=22½°; γ_0=14°; τ=3°.

The oscillatory acceleration is given in figures 6 to 9. These figures are the same as the figures giving the nodal acceleration (figs. 2 to 5), except that the acceleration plotted is the difference between the hull acceleration and the nodal acceleration. The time history of the hull acceleration can be obtained by summing the two plots for a particular mass ratio. On the basis of the assumption that during impact the airframe structure deflects in a particular mode, a time history of the acceleration of any point in the structure is obtained from the results for the equivalent two-mass system by the following procedure:

(1) From the deflection curve of the represented mode, obtain the ratio of the deflection of the point of interest to the deflection of the hull. Both deflections are taken relative to the nodal point.

(2) Multiply this ratio by the oscillatory acceleration given either by figure 6, 7, 8, or 9 or by interpolation between these figures for the mass ratio of the equivalent two-mass system.

(3) Add result to the nodal acceleration given by figures 2 to 5.

Time histories of the acceleration given in figures 2 to 9 are on a nondimensional basis. The nondimensional coefficients, which contain velocity, weight, fluid density, and acceleration of gravity, were used in reference 1 in a comparison of theoretical data with impact data for a float having an angle of dead rise of 22½°.

Application to other angles of dead rise.—The function of the angle of dead rise can also be included in the nondimensional coefficients, but in the present investigation this function is isolated and treated as a factor for correcting the results presented for angle of dead rise of 22½° to other dead-rise angles. The pertinent relationships between results for different angles of dead rise may be expressed as follows:

$$t \propto \left[\frac{1}{f(\beta)\, f(A)}\right]^{1/3} \tag{3}$$

$$n_p \propto [f(\beta)\, f(A)]^{1/3} \tag{4}$$

where

$f(\beta)$ function representing variation of virtual mass for two-dimensional flow with angle of dead rise

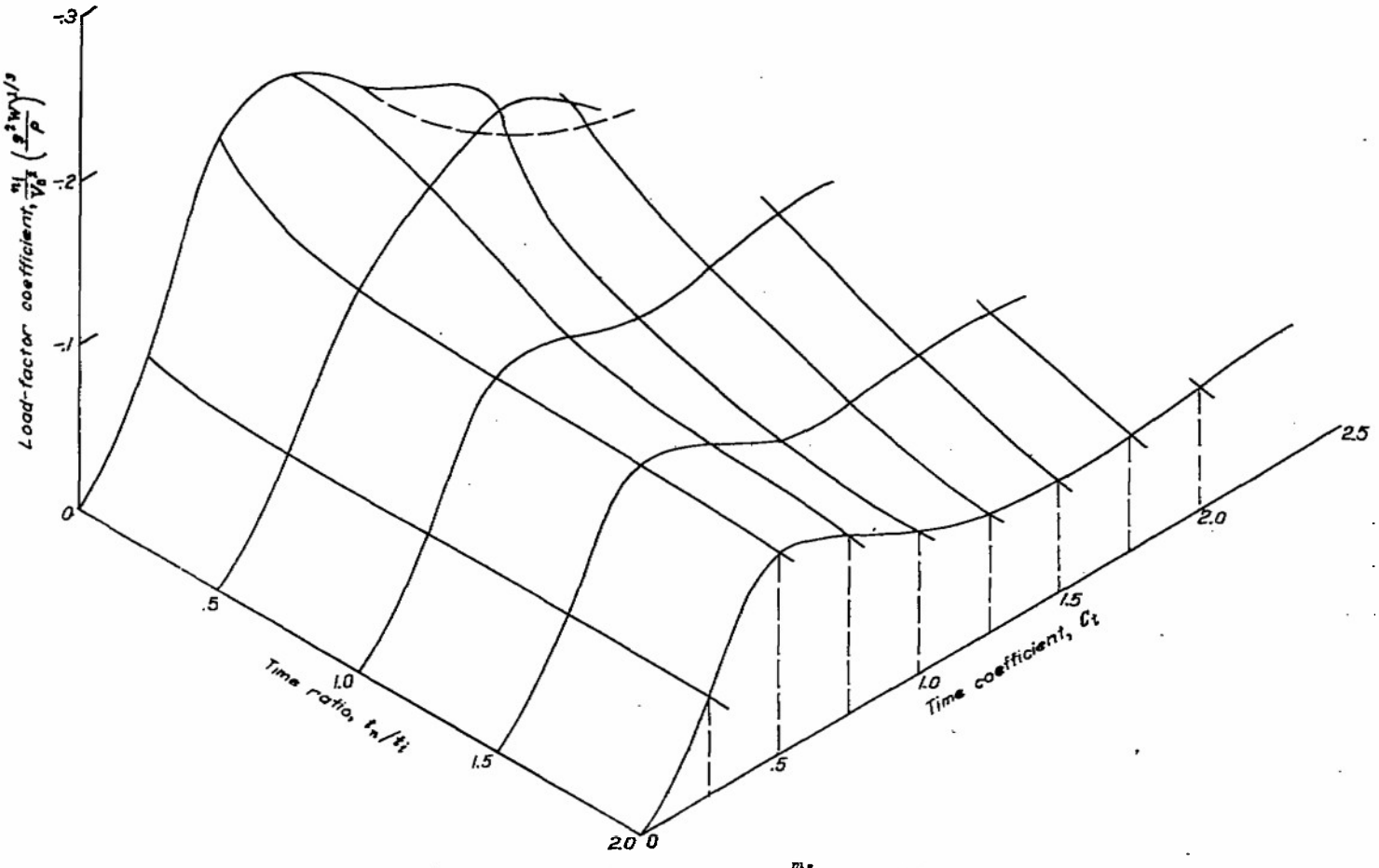

FIGURE 4.—Variation of force time history with time ratio. $\frac{m_s}{m_L}=1.00$; $\beta=22\frac{1}{2}°$; $\eta=14°$; $\tau=3°$.

$f(A)$ aspect-ratio factor including effect of angle of dead rise on aspect ratio; ratio of virtual mass for three-dimensional flow to virtual mass for two-dimensional flow

n_p acceleration at any point, either oscillatory, nodal, or total

The shape of the force and acceleration curves for a given value of t_n/t_i is independent of angle of dead rise, but the effect of angle of dead rise on t_i, as given by relation (3), does enter into the determination of the value of t_n/t_i for a particular solution. After the value of t_n/t_i for a particular solution has been determined, the acceleration and time values for an angle of dead rise of $22\frac{1}{2}°$ are proportioned by means of relations (3) and (4) to the corresponding values for the angle of dead rise used in determining t_n/t_i in order to obtain the proper acceleration history.

Although adequate impact data have not been available for checking the theoretical equations for angles of dead rise other than $22\frac{1}{2}°$, the theory is equally applicable to planing floats. Study of planing data has shown that the functions of angles of dead rise used in equations herein are approximately correct for angles of dead rise ranging from 15° to 30°. The functions are:

$$f(\beta)=\left(\frac{\pi}{2\beta}-1\right)^2 \tag{5}$$

$$f(A)=1-\frac{\tan\tau}{2\tan\beta} \tag{6}$$

Until improved functions of angles of dead rise are obtained, functions (5) and (6) should be substituted in equations (1) and (2) and in relation (4) to correct for angles of dead rise within the range from 15° to 30°. Rough approximation can be obtained by use of functions (5) and (6) for angles of dead rise greater than 30° but not for angles of dead rise much less than 15°. In reference 2 there is a discussion of the inadequacy of $f(A)$ for aspect ratios which normally occur for small dead-rise angles. For very large angles of dead rise and moderate velocity the static forces, which are not considered in the present investigation, become of greater importance.

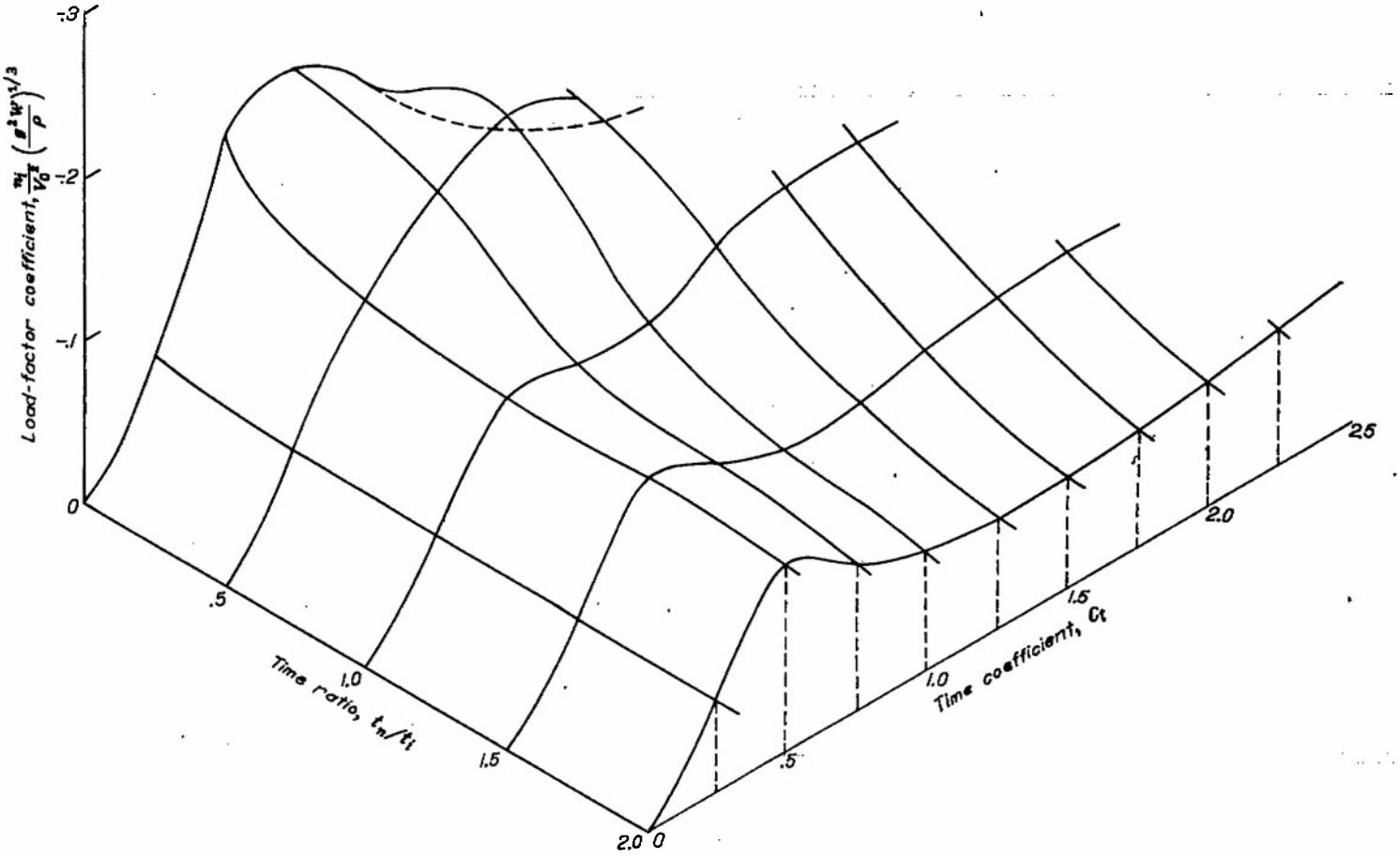

FIGURE 5.—Variation of force time history with time ratio. $\frac{m_s}{m_L}$=1.36; β=22½°; γ_0=14°; τ=3°.

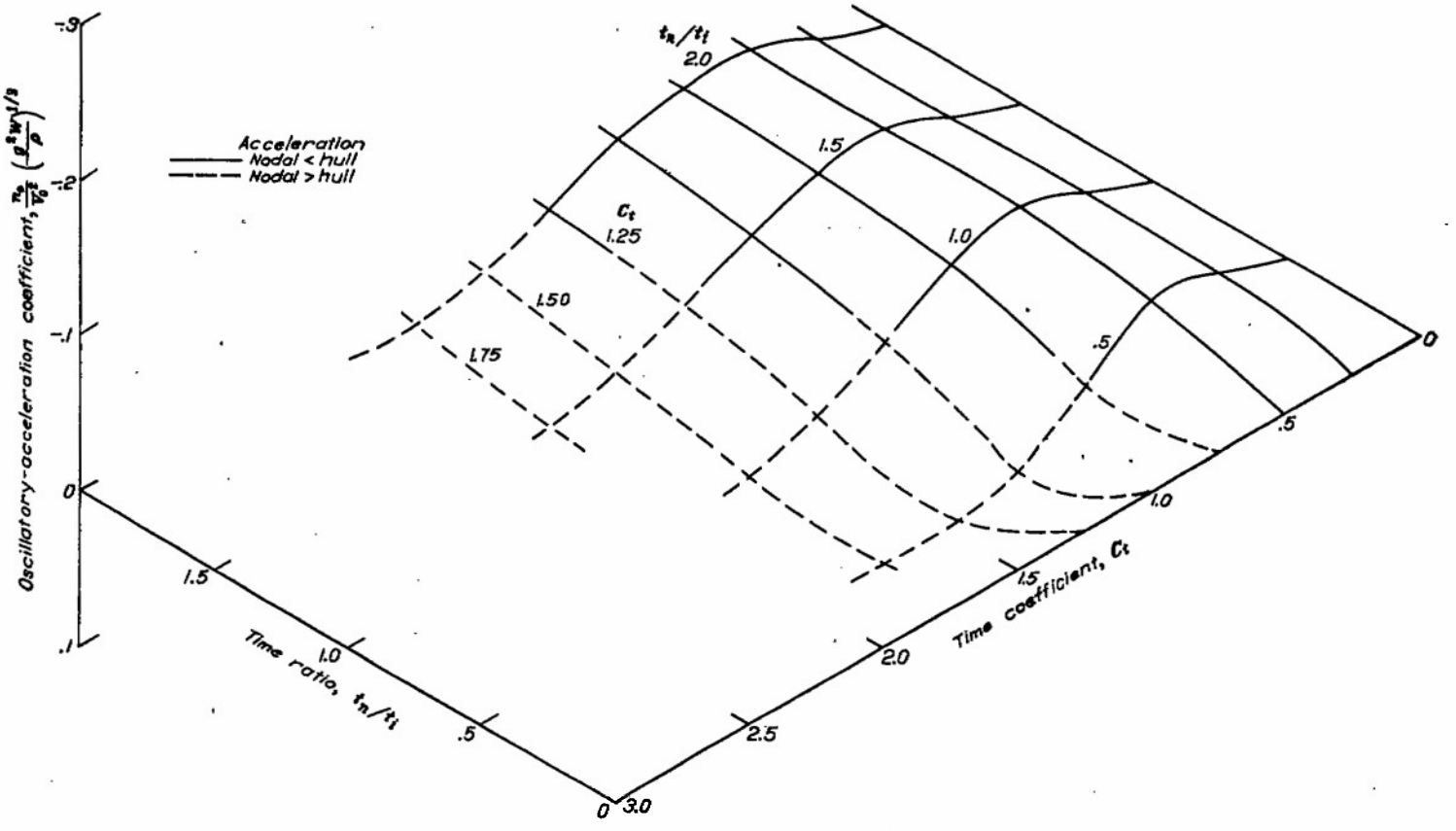

FIGURE 6.—Variation of oscillatory-acceleration coefficient with time ratio. $\frac{m_s}{m_L}$=0.25; β=22½°; γ_t=14°; τ=3°.

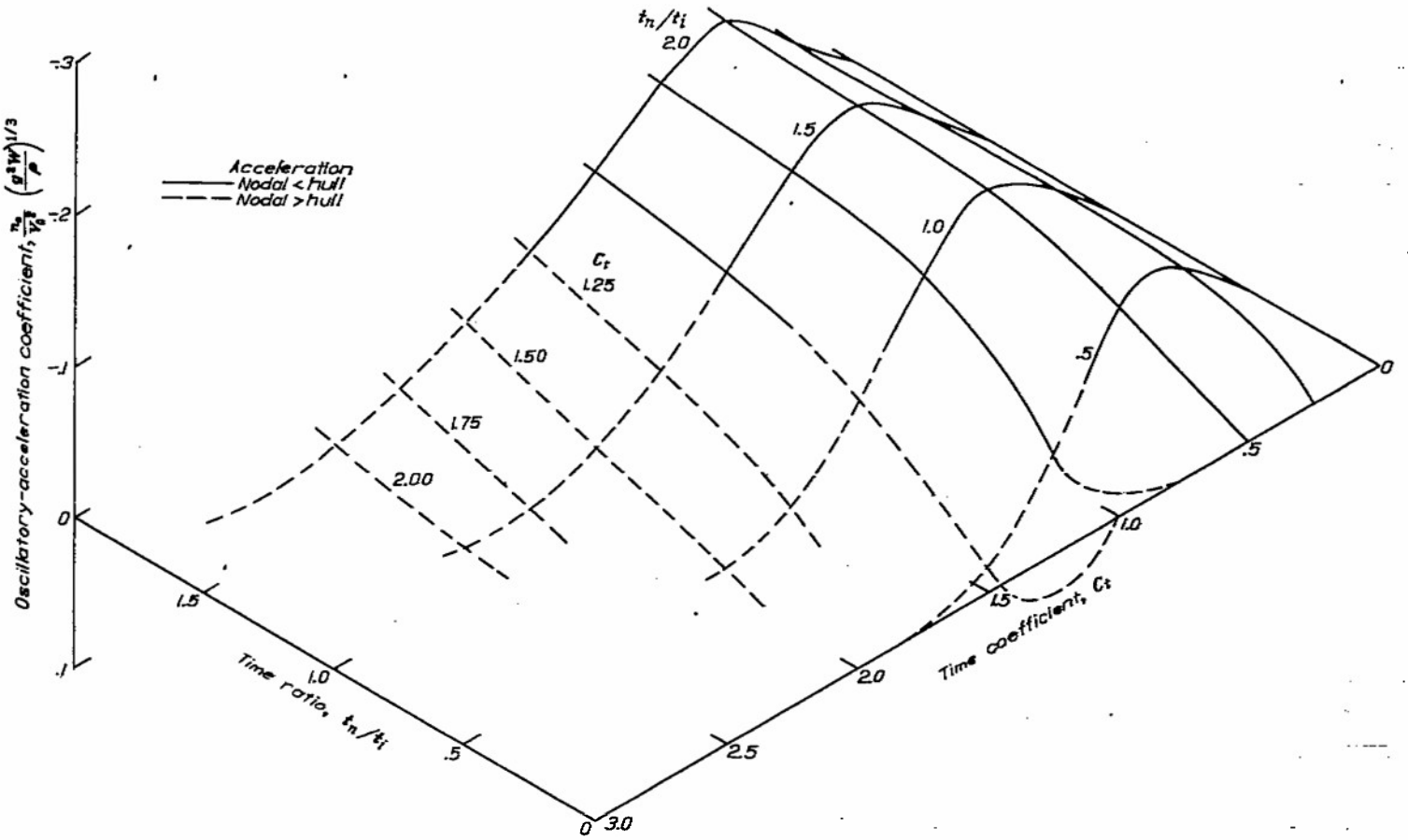

FIGURE 7.—Variation of oscillatory-acceleration coefficient with time ratio. $\frac{m_s}{m_L}=0.60$; $\beta=22\frac{1}{2}°$; $\gamma_1=14°$; $\tau=3°$.

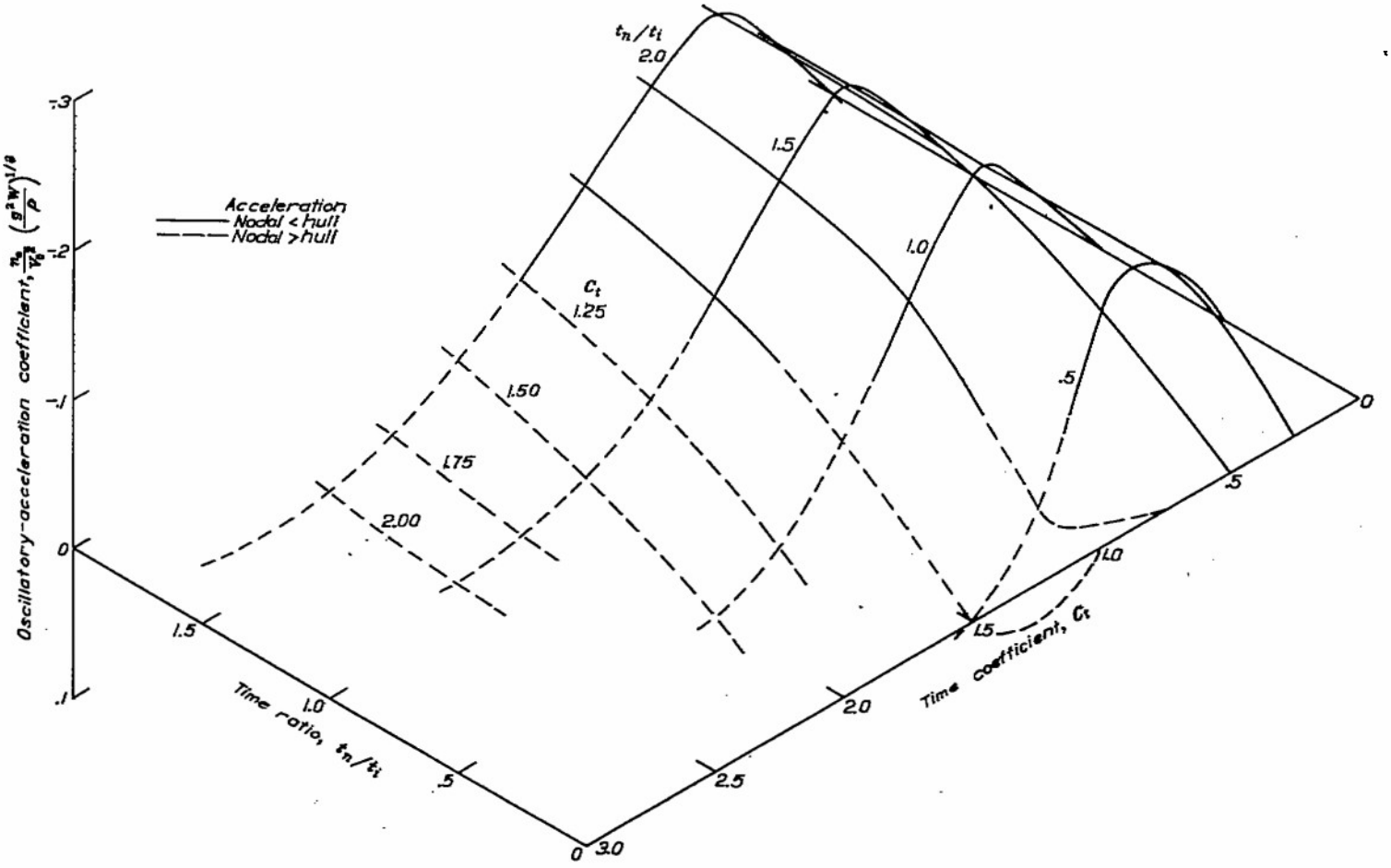

FIGURE 8.—Variation of oscillatory-acceleration coefficient with time ratio. $\frac{m_s}{m_L}=1.00$; $\beta=22\frac{1}{2}°$; $\gamma_1=14°$; $\tau=3°$.

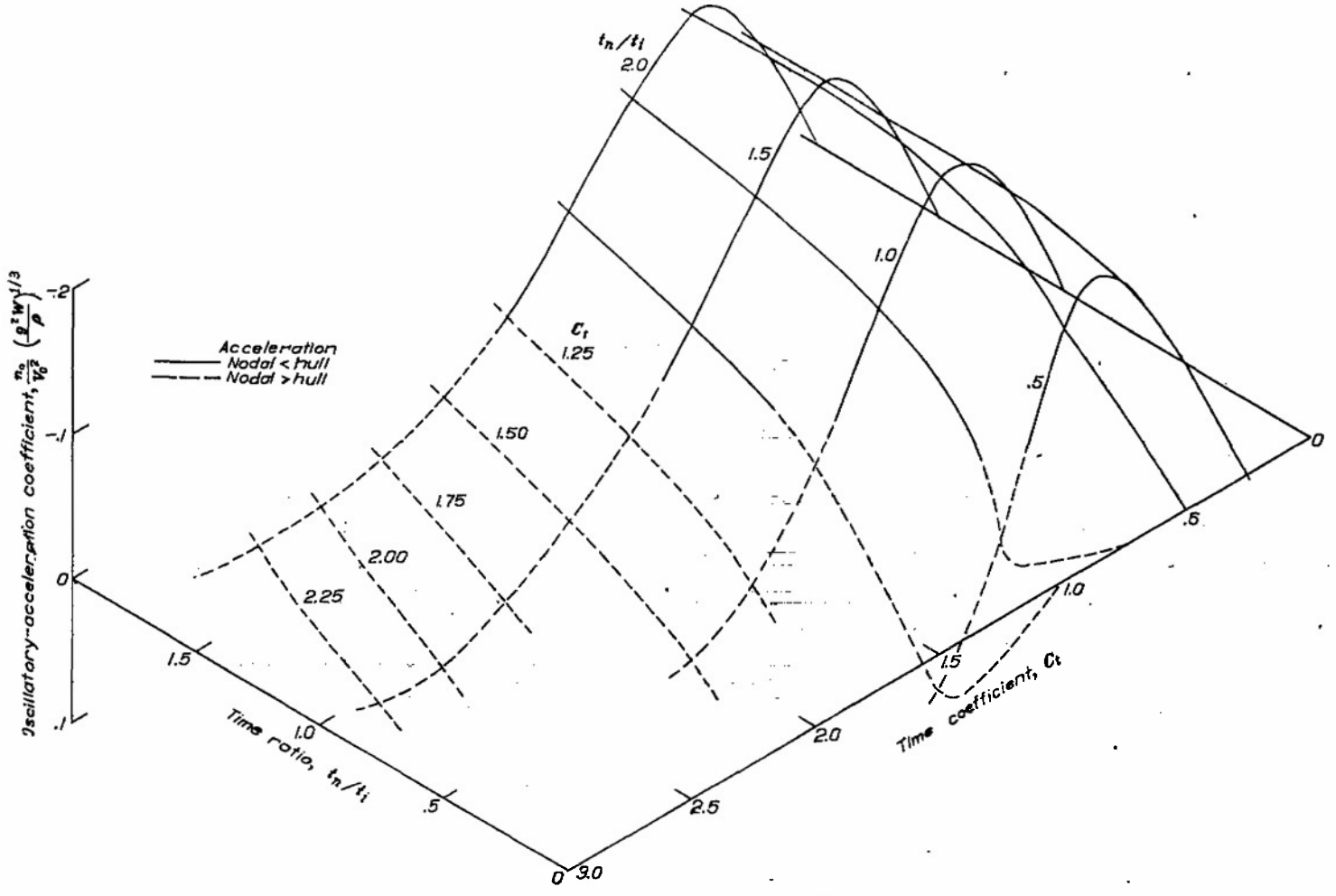

FIGURE 9.—Variation of oscillatory-acceleration coefficient with time ratio. $\frac{m_s}{m_L}=1.36$; $\beta=22\frac{1}{2}°$; $\gamma_1=14°$; $\tau=3°$.

Approximate correction to other flight paths and trims.—The flight-path and trim conditions of primary interest to the designer tend to be independent of the variables in seaplane design and constitute a limited range within which approximate correction of results to different angles of flight path and trims can be made without necessity for repeated time-history solutions. For any particular combination of horizontal speed, rate of descent, and trim, the most severe impact load for most of the structure occurs when the seaway is such that the keel contacts a wave slope approximately parallel to it. The effective angle of flight path and trim for such an impact are defined relative to the inclined wave slope; therefore, the trim which gives maximum force is zero. The largest flight-path angle, relative to the keel and to the critical wave slope, is also associated with the most severe force. The value of the largest flight-path angle is not so definite as the critical trim but tends to be independent of variations in size and wing loading. The velocity of the wave should be considered in determining the contact speed and flight-path angle.

The equations and method of solution given in appendix A permit solution for different flight-path angles and trims; however, approximate correction of the results in figures 2 to 9 to other positive contact angles can be made by assuming that the proportionate effect of the structural elasticity on the hydrodynamic force is solely dependent on the ratio t_n/t_i. Curves given in reference 1 show values of $C_{t_{a_{max}}}$ for different flight-path angles and trims, which may be substituted in equation (2) to obtain the value of t_n/t_i for different contact angles. In making the approximate correction, the solution presented herein for the obtained value of the ratio t_n/t_i should be used to approximate the shape of the curve giving the desired time history. The load or acceleration scale should be corrected to the different contact angles by multiplying the present result by the ratio, determined from curves given in both references 1 and 2, of the load-factor coefficient for the different contact condition to the load-factor coefficient for the conditions of 3° trim and 14° flight-path angle considered herein. Correction of the time scale involves a similar procedure in which the time coefficient is used rather than the load-factor coefficient.

Since the force curves for a rigid body are approximately the same shape for different angles of flight path and trims (reference 1), the approximate method of correcting to different angles of flight path and trims would be almost correct if the structural elasticity did not affect the hydrodynamic-force curve. The percentage change in the force on the float due to elasticity is a function of the percentage change

in draft caused by the elastic compression for a given center-of-gravity position. An indication of the validity of the approximate correction is obtained by studying the extent to which the ratio of the spring deflection to the draft is constant for impacts of the same values of t_n/t_i at different angles of flight path and trims. From the expressions for t_n/t_i, C_i, C_d, and C_t with the spring deflection assumed to be proportional to the hydrodynamic force, this ratio may be represented by the expression $C_iC_t^2/C_d$, in which all values are for the instant of maximum acceleration. The variation of this expression with flight path for an impact of a rigid float at 3° and 12° trim is given in figure 10. Values of C_i and C_t used in obtaining this figure are given in reference 1; values of C_d were obtained in conjunction with the data of reference 1 but have not been published.

In the present report the numerical values of $C_iC_t^2/C_d$ have no significance and they are of interest only because of the extent to which they are constant. Figure 10 indicates that for large flight-path angles and small trims the ratio is approximately constant. The deviation from a constant value of this ratio is due to planing forces which exist in an oblique impact and become more important for low flight-path angles and high trims. The conditions of large flight-path angle and small trim previously adjudged to be of primary interest to the designer constitute the ranges in which the deflection ratio is fairly constant and the approximate method of correction should give a fair degree of accuracy. The present solutions are considered to be for conditions suited to correction of the results to other conditions of greatest practical interest; they represent a moderately severe combination of flight-path angle, wave slope, and trim chosen to facilitate correlation of the theory with an impact which resulted in substantial damage to a well-instrumented flying boat during flight tests.

The equations presented herein are not valid for zero trim; an assumption that the float is prismatic gives solutions of infinite wetted length and infinite force for zero trim. Solution for 3° trim and a prismatic float is much simpler than a correct solution for 0° trim because necessity for consideration of bow shape is eliminated. The solution for 3° trim may be taken as an approximation of the critical design load or, as illustrated in the following section in a comparison of theory with experiment, an empirical factor, which includes bow effects, may be used to convert values of acceleration and time for 3° trim to values for 0° trim.

COMPARISON WITH EXPERIMENT

Impact basin data have not been obtained for suitable models, and most flight landing data have been inadequate for the present study. The only data which appeared suitable for this comparison are those which were obtained with a four-engine flying boat, the data for which have not been published. Data were obtained for a large number of test landings, but only one of the impacts is very well suited to the present analysis. This impact gave loads sufficiently high to cause large effects of elasticity of the wings. The impact occurred against the flank of a sizable wave (4 ft)

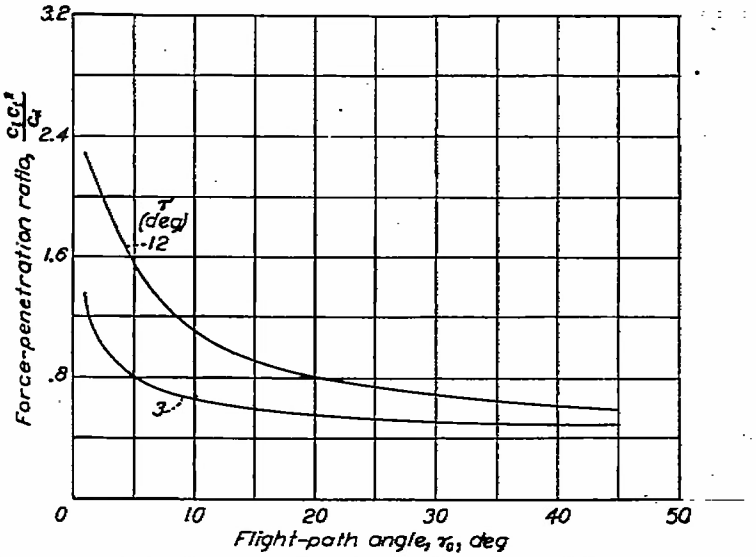

FIGURE 10.—Variation of force-penetration ratio at maximum force with flight-path angle and trim.

and thus facilitated the use of results based on a planar water surface. The present comparison of theory with experiment will be restricted to this impact since other impacts involved more complex contact with seaway and gave less force.

The horizontal speed, rate of descent, and trim were recorded. A large number of pressure instruments distributed in the hull permitted determination of the water surface relative to the hull. Data recorded by these instruments indicated that the wave slope in contact with the hull was approximately planar, that the trim relative to the wave slope was 0°, that the resultant velocity, considering the speed of the wave, was 85 feet per second, and that the flight-path angle relative to the wave slope was 14°.

Structural data available for the test flying boat are not adequate for the present analysis. Since this flying boat has the same number of engines and approximately the same gross weight and horsepower as a landplane for which a large amount of structural data is available, assumption is made that the flying-boat wing has the same mode shape and mass distribution as the wing of this landplane. Use in equation (B6) in appendix B of data for the landplane given in reference 3 leads to the following mass ratio of the two-mass system representing the fundamental mode:

$$\frac{m_s}{m_L}=0.25$$

Based on study of the accelerations at several points in the test flying boat during periods of relatively free vibration in which the fundamental wing bending mode appeared to be predominant, a natural frequency of 3.6 cycles per second was selected for use in the present example. The fundamental mode frequency of the wing of the landplane is 3.4 cycles per second. (See reference 3.)

Since the mass ratio is equal to 0.25, figures 2 and 6 are used to approximate the action of the fundamental mode. Further, substitution of values for conditions for this impact in equation (2) results in use of the specific time history

given for $\frac{t_n}{t_i}=1.2$. Substitution of the contact conditions in the load and time coefficients fixes the load and time scales in an absolute sense. Correction from 3° trim to 0° trim may be made by assuming that the shape of the time history is approximately the same for both conditions. Empirical correction of the curves from 3° trim to 0° trim may be seen from reference 2 to require a 10-percent reduction in the acceleration. An analysis of data obtained at the Langley impact basin for impact at 0° trim indicates that correction of the time scale from 3° trim to 0° trim requires a 10-percent reduction in the time values.

Hydrodynamic force.—The nodal-point acceleration n_i, obtained by the procedure discussed herein, represents the hydrodynamic force, in multiples of the weight, applied to the flying boat. Since the experimental data do not provide measurement of the hydrodynamic force as such, direct comparison of the theoretical force-curve results with experimental results is not permitted. Instead, a comparison of the theoretical response of the structure with the experimental response is necessary, and, if the agreement is adequate, it may be concluded that both the hydrodynamic and the structural actions are adequately represented.

Before a study of the response of the structure is made, the theoretical effect of the response on the hydrodynamic force should be observed. This observation is made by comparing the force curve obtained for a mass ratio of 0.25 with the force curve for a rigid structure. Both curves are included in figure 11. The curve for the case of a rigid structure $\left(\frac{m_s}{m_L}=0\right)$ was obtained from reference 1 for 3° trim and corrected to the conditions of the present example as previously indicated. Comparison of the curves for mass ratios of 0 and 0.25 shows that in the present example the theoretical effect of the structural elasticity on the maximum hydrodynamic force is to reduce it 15 percent. For the hypothetical condition of a concentrated wing mass located at a point in each semispan of a massless wing structure, the conditions of the present example would give theoretical reduction in the maximum hydrodynamic force due to structural elasticity of 44 percent. This result is indicated by comparison of the maximum of the curve in figure 11 for a mass ratio of 1.36 with the maximum of the curve for mass ratio of 0.

The curves in figure 11 show only reduction of the hydrodynamic force because of structural elasticity. It should not be concluded, however, that the effect is always in this direction. Figures 2 to 6 show that in some cases the hydrodynamic force is increased; the maximum increase which was calculated was of the order of 12 percent.

Hull acceleration.—By combining the results for the two-mass case with approximation of the pitching action on the basis of a rigid structure, the following equation may be obtained for the hull acceleration at different longitudinal stations:

$$n_h=n_i f+n_e \tag{7}$$

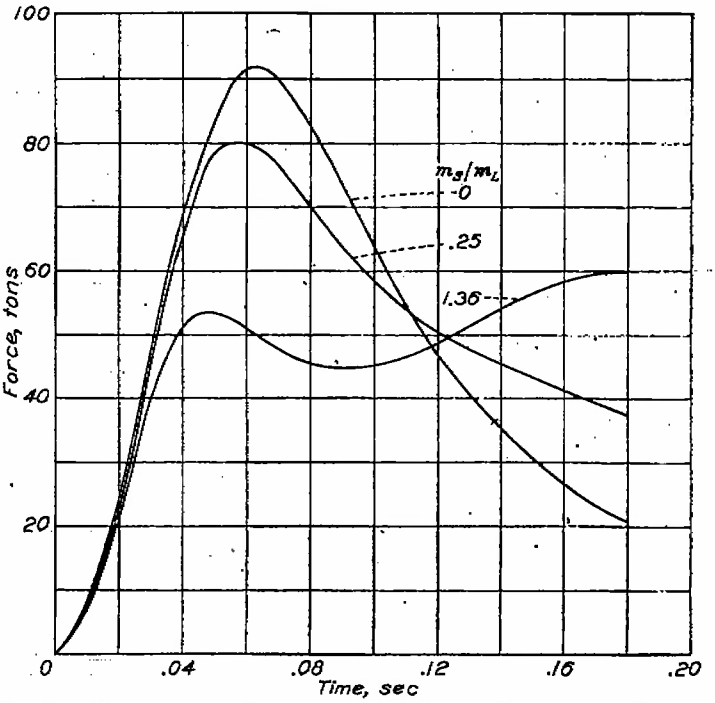

FIGURE 11.—Variation of hydrodynamic force with time. $\tau=0°$; $\gamma_0=14°$; $V_i=88$ feet per second; $W=40{,}000$ pounds; $f_n=3.6$ cycles per second.

where

n_h hull acceleration

$f=1+\frac{sl}{k^2}$

s distance from station to center of gravity

k radius of gyration (12 ft in present example)

l distance from resultant hydrodynamic force to center of gravity.

The forebody length of the flying boat is 31.75 feet. Because of bow effects, a length of 25 feet is assumed to have a rectangular loading for this zero-trim impact and the resultant force is located 12.5 feet forward of the step which leads to a value of l equal to 8 feet. Use of the foregoing procedure to calculate time histories of the acceleration for two stations in the hull at which accelerometers were located gives the curves in figure 12. The maximum accelerations recorded at these stations are also shown; agreement with the computed maximum acceleration is good. The full experimental time history is not included because the film speed was not great enough to permit accurate determination of the shape of the time history. This factor, together with some uncertainty in defining the exact instant of contact, prevents exact check of the time to reach maximum acceleration; thus, the experimental points in figure 12 are located at the theoretical time of maximum acceleration.

Although the agreement of calculation with experiment in figure 12 is good, this agreement can be interpreted as confirmation of the elastic action of the structure only to the extent that disagreement of hull accelerations computed on the basis of a rigid structure can be shown. Values of maximum accelerations computed for a rigid structure are included in figure 12. The disagreement with experiment

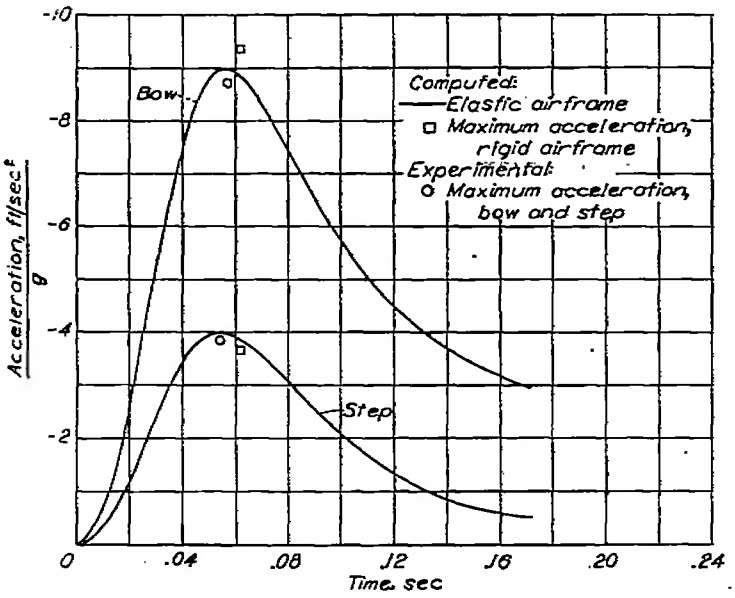

FIGURE 12.—Variation of bow and step acceleration with time.

is greater than for computations in which the elasticity of the structure is considered. The difference is small, however, because the effect of elasticity in increasing the hull acceleration for a given force is largely offset by the effect of elasticity in reducing the hydrodynamic force. Since the probable accuracy of available data must be considered, experimental proof of the theoretical effect of the elasticity on the hull acceleration cannot be claimed. Support for a conclusion in this respect, however, can be obtained by comparing the theoretical response of the wing with the experimental response. If the wing responds as assumed, the basic equations require that the hydrodynamic force and hull accelerations be as calculated.

Elastic axis.—Use of the nodal and oscillatory accelerations of the representative two-mass system to predict accelerations along the elastic axis of the wing requires consideration of the fact that the elastic axis of the wing is not at the center of gravity of the flying boat. An approximate correction may be obtained by multiplying the results for the two-mass case by the factor f which is used in equation (7). This correction is not entirely consistent with that given by equation (7), but each approximation is considered more accurate for its particular case. An improvement to the present correction which would change the results 2 to 3 percent might be made, but the complication is not considered to be warranted.

In the present example the value of f is 0.86. Application of this factor, of equation (B7) of appendix B, and of pertinent structural data given in reference 3 gives the curves in figure 13 in representation of the acceleration time histories of the elastic axis of the wing for the hull, inboard-engine, nodal, outboard-engine, and tip stations.

Wing torsion.—The torsion of the wing during impact may have substantial effect on the acceleration of engine and nacelle masses forward of the wing. Use of the procedure which gave the acceleration time histories in figure 13 to calculate the acceleration at the engine gives a maximum acceleration of $3g$ at the inboard engines and a maximum acceleration of $5.6g$ at the outboard engines. The relative magnitude of these values is in strong disagreement with the fact that during this impact partial failure of the inboard-engine mounts occurred, but the outboard-engine mounts were not damaged.

Since the structural data used in the preceding computation are for the actual fundamental mode, their use in impact calculations involves assumption that the coupling between the torsion and bending corresponds to the coupling which exists in natural vibration. Actually, the torsional deflections in impact are determined not merely by the bending deflections but also by the large nodal acceleration, which does not exist in natural vibration.

In the present example the results which have been calculated for impact of a two-mass elastic system will be used to predict the response of the engines. The procedure for doing this is to select the proper solution and then to adjust the acceleration and time scales of the two-mass solution so that the maximum acceleration of the nodal point corresponds to the maximum acceleration of the elastic axis at the engine station. The acceleration of the upper mass of the two-mass system then represents the response of the engines; however, because of the eccentricity of the impact, an increment must be added.

Data obtained from Guggenheim Aeronautical Laboratory, California Institute of Technology include the torsional deflection of a station inboard of the outboard engine for a given moment applied at the wing tip. For a flying boat the absence of cut-out for the landing gear tends to give a stiffer wing; therefore, in the present example, deflection measured on the wing of the landplane slightly inboard of the outboard engine is considered applicable to the outboard-engine station. Relative deflections between the inboard and outboard engines are estimated as follows:

(1) Torsional deflection at inner engine equal to 1 unit due to each engine, or 2 units total

(2) Torsional deflection between inboard and outboard engines equal to 2 units because of greater distance of flexure, boosted to 3 units because of increased flexibility of structure.

On the basis of data from California Institute of Technology the average of the static moments of the inboard and outboard engines is taken as 22,000 foot-pounds. After determination of the torsional deflection at the outboard engine for this average moment applied at the wing tip, multiplication by the ratio 1/2 gives a value for the static deflection of the inboard engine and multiplication by the ratio 5/4 gives a value for the static deflection of the outboard engine.

An approximation to the calculation of the response of the engines to the total acceleration of the elastic axis is to neglect dynamic interaction between the engines and treat each engine as a single-mass oscillator having a natural frequency determined by its static deflection. Such a procedure gives values of 7.6 cycles per second for the inboard engine and 5.1 cycles per second for the outboard engine. Use of these frequencies to determine t_n and division of t_n by

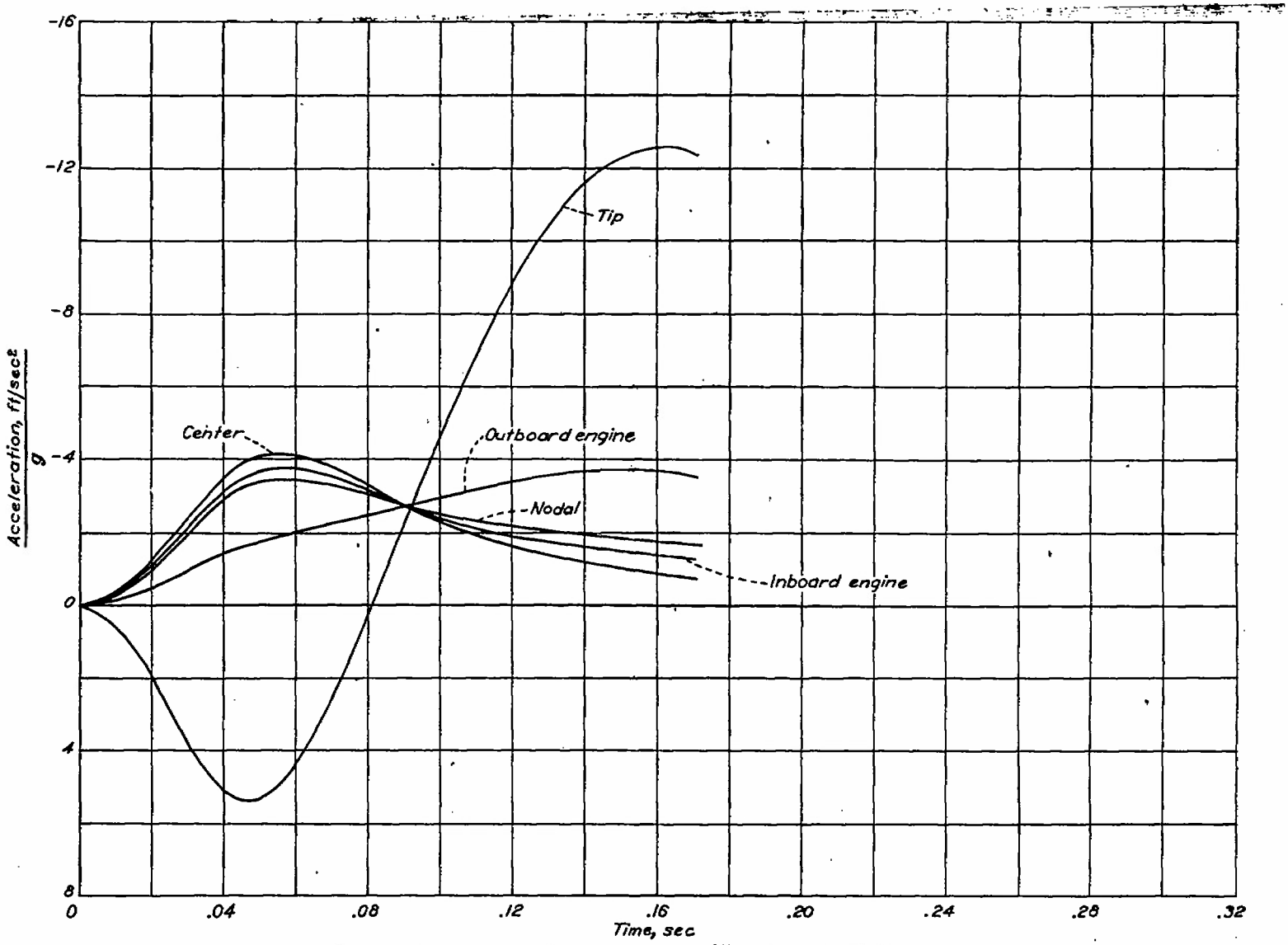

FIGURE 13.—Variation of accelerations at stations along the wing elastic axis with time.

t_t (t_t equal in this case to the time to reach maximum acceleration of the curves in figure 13 for the station in question) leads to values of t_n/t_t for the inboard and outboard engines. The next step is to select a mass ratio which for these values of t_n/t_t has a shape of the nodal acceleration time history, which approximates the shape of the acceleration time history for the elastic axis at the station in question. In the present example the mass ratio of 0.25 is used. Scale factors for both the load and time scales are determined so that the maximum nodal acceleration for the two-mass solution will agree with the maximum acceleration and time to reach maximum acceleration of the elastic axis at the station in question. After these factors are applied to both the nodal and oscillatory curves for the selected mass ratio and time-period ratio, use of the results and equations (B7), (B5), and (B2) in appendix B to calculate the acceleration of the sprung mass of the two-mass system gives accelerations of the engines. Approximation and superposition of the pitching action on the basis of a rigid structure leads to the solid-line curves given in figure 14 for the accelerations of the engines.

Also included in figure 14 is the design ultimate acceleration for the engine mounts. Comparison of the calculated engine accelerations with this value shows agreement of the calculation with the fact that partial failure of the inboard-engine mounts occurred but the outboard-engine mounts were not damaged.

During the impact an accelerometer was located at the outboard-engine station intermediate between the elastic axis and the engine. A calculated time history of the acceleration at the accelerometer location is given in figure 14; this time history is based on linear interpolation between the computed accelerations at the engine and the elastic axis at this station in accordance with the proportionate distances involved. The figure also includes the recorded maximum acceleration at this point and shows good agreement of the computed acceleration therewith.

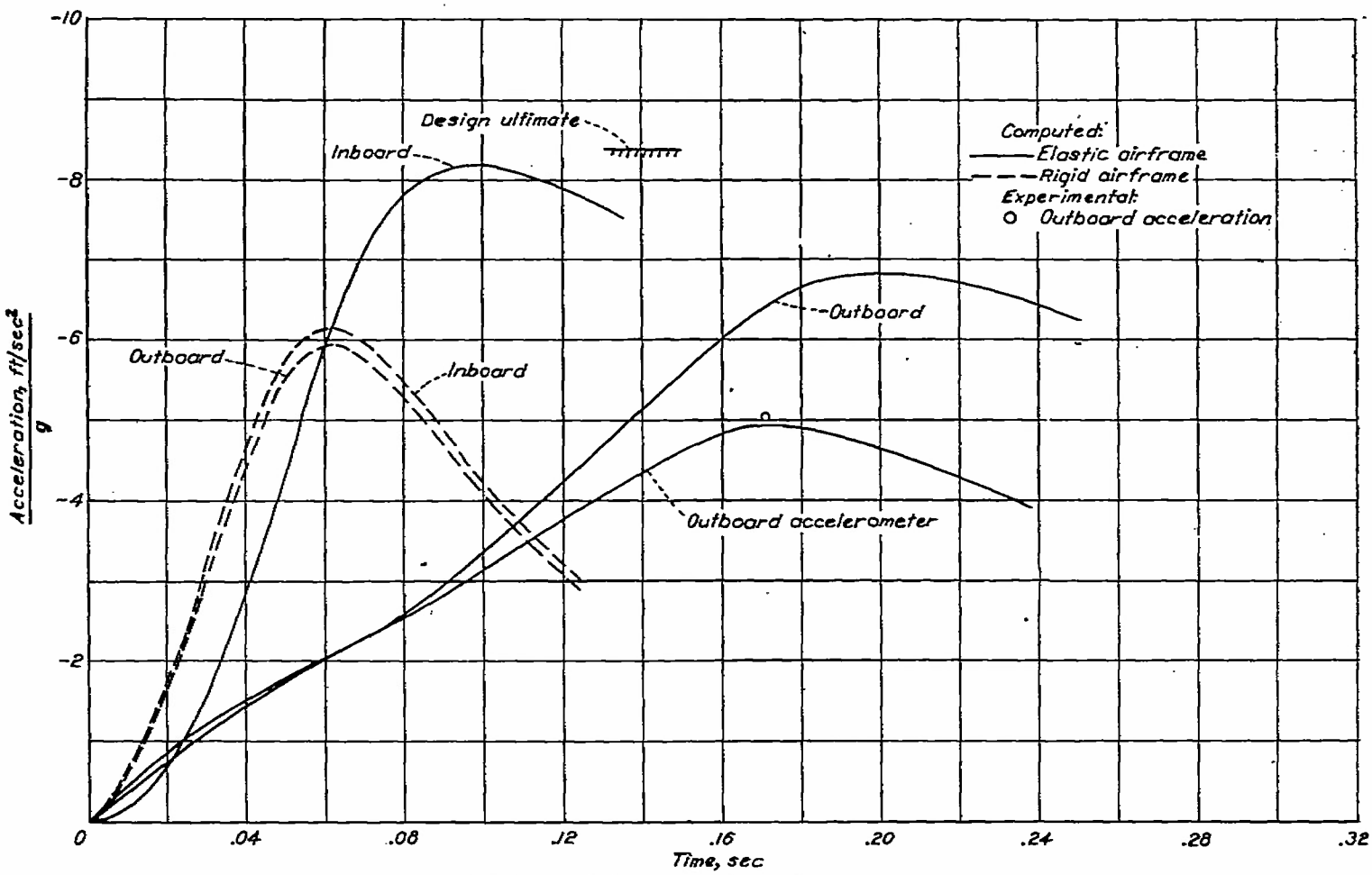

FIGURE 14.—Variation of accelerations of engines with time.

Acceleration time histories for the engines, computed on the basis of a rigid structure, are included in figure 14. The maximum accelerations computed on this basis do not agree with the structural failures which occurred. Furthermore, the fact that the curves computed on the basis of a rigid structure reach a maximum at the same instant of time is in strong disagreement with experiment, which in this respect is in approximate agreement with the computations for an elastic structure.

Difference between the ratio t_n/t_i for the inboard-engine and outboard-engine stations is primarily responsible for difference in the calculated response of the engines. Most of the difference in this ratio for the two stations is not due to difference in the sprung-engine frequency but is due to the greatly different time to reach maximum acceleration t_i of the elastic axis. Agreement with experiment of the response calculated at these stations provides indirect confirmation of the acceleration time histories predicted for the elastic axis at these locations by the normal-mode method.

For the impact, experimental data are not available for checking the tip acceleration, which is predicted on the basis of the normal-mode method, but the initial downward acceleration and the $12g$ maximum acceleration shown in figure 13 for this station are in general agreement with results recorded in severe impacts of other airplanes. Agreement of the computed hull acceleration with experiment has already been shown; in an indirect manner all the curves in figure 13 exhibit satisfactory agreement with available experimental data. Although the response of the engines is different from the response assumed in calculating these curves, it appears that in practical use the two-mass solutions given herein can be interpreted on the basis of the normal-mode method to obtain both the response of the elastic axis and the hydrodynamic force. Further, it appears that in practical problems modification of these two results is not required when accelerations of the engine different from the accelerations predicted by the normal-mode method are determined; the merit of this statement should be independent of whether such modification is made by the method used herein or by another method.

In the foregoing comparison agreement of calculation with experiment is obtained without consideration of the response of modes higher than the fundamental mode. If, when more data are available, it is shown that the response of the higher modes can be determined by treatment parallel to that given the fundamental mode, the two-mass solution

given herein can be used to predict their response by selecting a solution, for a mass ratio and natural frequency representative of the higher mode, which has a nodal acceleration curve of approximately the same shape as the hydrodynamic-force curve.

CONCLUSIONS

Theoretical solution of hydrodynamic impact of a hull mass connected by a spring to an upper mass, the results of calculations for wide ranges of mass ratio and natural frequency, and the use of these results in a comparison of theoretical data with test data for a flight-test landing impact indicated that:

1. In flying-boat impact the effect of the structural response on the hydrodynamic force might be substantial, the shape of the force time history might be considerably changed, and the maximum hydrodynamic force might be either reduced or increased.

2. The greatest reduction in hydrodynamic force occurred for the condition of large mass ratio and low value of spring constant.

3. The normal-mode method was a practical means for determining the equivalent two-mass system which represented the major elastic action of the airframe, for predicting the effect of this action on the hydrodynamic force, and for approximating accelerations along the elastic axis of the wing.

4. The acceleration of engines contained in nacelles forward of the wing could not be computed on the basis of coupling between torsion and bending as in the fundamental mode, but simple treatment of their response to the combined translation and oscillation of the elastic axis gave agreements with experimental accelerations and gave an explanation of partial failure of the inboard-engine mounts during impact.

LANGLEY MEMORIAL AERONAUTICAL LABORATORY,
NATIONAL ADVISORY COMMITTEE FOR AERONAUTICS,
LANGLEY FIELD, VA., *March 17, 1947.*

APPENDIX A

MATHEMATICAL EQUATIONS AND METHOD OF SOLUTION

EQUATIONS OF MOTION

The following equations of motion, which were derived from equation (30) in reference 2, are for fixed-trim impacts of a rigid prismatic float connected by a massless spring to a rigid upper mass:

Acceleration of lower mass normal to water surface in feet per second per second

$$-\ddot{y}_L=\left\{3Ay_L^2(\dot{y}_L+K_1\cos\tau)^2+\frac{K}{m_S}\left[\frac{Ay_L^4}{4}+(m_S+m_L)(y_L-\dot{y}_{L_0}t)+2K_1A\cos\tau\int_0^t y_L^3dt+3AK_1^2\cos^2\tau\int_0^t\int_0^t y_L^2dt\,dt\right]\right\}\frac{1}{Ay_L^3+m_L} \tag{A1}$$

Acceleration of sprung mass normal to water surface in feet per second per second

$$\ddot{y}_S=\frac{1}{m_S}[(Ay_L^3+m_L)\ddot{y}_L+3Ay_L^2(\dot{y}_L+K_1\cos\tau)^2] \tag{A2}$$

Acceleration of nodal point normal to water surface in feet per second per second

$$\ddot{y}_n=\frac{m_L\ddot{y}_L+m_S\ddot{y}_S}{m_L+m_S} \tag{A3}$$

The spring constant in pounds per foot of deflection can be expressed by the equation

$$K=\frac{4\pi^2(m_Lm_S)f_n^2}{m_L+m_S} \tag{A4}$$

where

$$K_1=\dot{x}_{L_0}\sin\tau-\dot{y}_{L_0}\frac{\sin^2\tau}{\cos\tau}$$

$$A=0.82\left(\frac{\pi}{2\beta}-1\right)^2\left(1-\frac{\tan\tau}{2\tan\beta}\right)\left(\frac{\pi\rho}{6\sin\tau\cos^2\tau}\right)$$

$\ddot{y}_L$ velocity of lower mass normal to water surface, ft/sec
y_L draft normal to water surface, ft
β angle of dead rise, radians
τ angle of trim, deg
$\dot{y}_{L_0}$ initial velocity normal to water surface, ft/sec
$\dot{x}_{L_0}$ initial velocity parallel to water surface, ft/sec
m_S sprung mass, slugs
m_L lower mass, slugs
f_n natural bending frequency, cycles/sec
ρ mass density of water, slugs/cu ft

COMPUTING DIRECTIONS

A sample data sheet is given as table I. In this table the numbers in circles refer to rows; the circled numbers under the row headings refer to computed values to be used for the computations. In the first column the time is equal to zero, in the second column the time is Δt, and in successive columns the time is 2 Δt, 3 Δt, and so forth. Each row is computed in sequence for any given column before any row is computed for the next column, except for the first column.

TABLE I.—DATA SHEET—GENERAL TERMS

Row	Row heading	Column 1	2	3	4
①	Time, sec				
②	㉒$_p=\dot{y}_L$, assumed				
③	(㉒$_p\times\Delta t$) + ③$_p=y_L$, ft				
④	③$^2=y_L^2$				
⑤	③$^3=y_L^3$				
⑥	③$^4=y_L^4$				
⑦	(②+$K_1\cos\tau$)^{2}④$\times 3\pi$				
⑧	⑥$\times\frac{A}{4}$				
⑨	(m_L+m_S)(②$-\dot{y}_{L_0}\times$①)				
⑩	$\left[(⑤+⑤_p)\frac{\Delta t}{2}\right]+⑩_p=\int_0^t y_L^3dt$				
⑪	$2K_1A\cos\tau\times$⑩				
⑫	$\left[(④+④_p)\frac{\Delta t}{2}\right]+⑫_p=\int_0^t y_L^2dt$				
⑬	$\left[(⑬+⑬_p)\frac{\Delta t}{2}\right]+⑬_p=\int_0^t\int_0^t y_L^2dt\,dt$				
⑭	$3AK_1^2\cos^2\tau\times$⑫				
⑮	⑧+⑨+⑪+⑭				
⑯	$\left(\frac{K}{m_S}\times$⑮$\right)$+⑦				
⑰	($A\times$⑤)$+m_L$				
⑱	$-\frac{⑮}{⑰}=\ddot{y}_L$, ft/sec^2				
⑲	(⑱+⑱$_p$)$\frac{\Delta t}{2}$				
⑳	⑲+⑳$_p$				
㉑	$\dot{y}_{L_0}$+㉑				
㉒	㉑+$\frac{⑲}{2}$				
㉓	㉒+$\frac{⑲}{2}$, $\dot{y}_L$ assumed for next interval				
㉔	$\frac{\left[-\frac{1}{m_S}(⑦-⑮)\right]}{32.2}=\ddot{y}_S$, g units				
㉕	$\frac{⑱}{32.2}=\ddot{y}_L$, g units				
㉖	$\frac{(m_L\times$㉕$)+(m_S\times$㉔$)}{m_L+m_S}=\ddot{y}_n$, g units				

In the first column the assumed value of $\dot{y}_L$ is the given value of $\dot{y}_{L_0}$. All other values are zero except the values for rows ㉑, ㉒, and ㉓ which in this case are also $\dot{y}_{L_0}$. Lower-case p as a subscript on a row number refers to the computed value in the indicated row of the preceding column.

Each row heading indicates the general operation to be performed. When the data sheet is set up, numerical values should be substituted in the row headings for the expressions that are constant for a specific case. The constants for the sample computation, given in table II, are as follows:

K	107, 664
K_1	4. 24317
A	133. 919
β, deg	22.5
τ, deg	.3
$\dot{y}_{L_0}$, ft/sec	20. 6673
$\dot{x}_{L_0}$, ft/sec	82. 1585
m_S	715. 217
m_L	525. 776
f_n, cycles/sec	3
ρ, slugs/cu ft	1. 938
Δt, sec	0. 005

For most solutions a time increment Δt of 0.005 second is satisfactory. (The value of Δt may be varied by considering the time for a given mass to reach a maximum acceleration.)

The number of significant figures to be used should be chosen on the basis of the computing equipment available and the accuracy desired. Comparison of a solution computed with four significant figures with results which had been obtained with six significant figures gave a difference of about 1 percent in the maximum acceleration.

As the computations proceed, the lower-mass acceleration (row ㉕), the sprung-mass acceleration (row ㉔), and the nodal-point acceleration (row ㉖), all in g units, should be plotted against time (row ①) in seconds. Each time a column is completed the new points should be added to the plot. This plot is the only brief method of checking on the accuracy of the computation until sufficient solutions are obtained to permit cross-plotting. If the points do not lie on a smooth curve, an error has been made in the computations. If an error is made, every value computed thereafter contains the error and therefore great care must be taken.

The number of columns required for the computations depends on the number of columns required for rows ㉕ and ㉔ to pass their respective maximums. At least three columns should be computed beyond the column in which row ㉔ reaches its maximum value.

TABLE II.—SAMPLE COMPUTATION

[Constants are from appendix A]

Row	Row heading	Column 1	2	3	4	5	6	7	8
①	Time Δt, sec (0.005)	0	0. 005	0. 010	0. 015	0. 020	0. 025	0. 030	0. 035
②	㉒$_p$	20. 6673	20. 6673	20. 6420	20. 5287	20. 2688	19. 8290	19. 1964	18. 3859
③	(㉒$_p$×0.005)+㉓$_p$	0	0. 103337	0. 206579	0. 309380	0. 411128	0. 511025	0. 608174	0. 701700
④	③^2	0	0. 010679	0. 042675	0. 095716	0. 169026	0. 2611147	0. 369876	0. 492383
⑤	②^2	0	0. 001104	0. 008816	0. 029613	0. 069491	0. 133453	0. 224949	0. 345505
⑥	③^4	0	0. 000114	0. 001821	0. 009162	0. 028570	0. 068198	0. 136808	0. 242441
⑦	(③+4.23736)^4×401.757	0	2661. 07	10612. 5	23586. 5	40782. 0	60767. 4	81602. 9	101246. 0
⑧	⑥×33.4798	0	0. 003817	0. 060967	0. 306742	0. 956518	2. 28326	4. 58030	8. 11688
⑨	1240.99[⑧−(20.6673×①)]	0	0	−0. 116653	−0. 781824	−2. 75252	−7. 02152	−14. 8995	−26. 8749
⑩	[(⑤+⑤$_p$)0.0025]+⑩$_p$	0	0. 000003	0. 000028	0. 000124	0. 000373	0. 000879	0. 001775	0. 003201
⑪	1134.92×⑩	0	0. 003405	0. 031778	0. 140730	0. 422190	0. 997595	2. 01448	3. 63288
⑫	[(④+④$_p$)0.0025]+⑫$_p$	0	0. 000027	0. 000160	0. 000506	0. 001168	0. 002243	0. 003821	0. 005977
⑬	[(⑫+⑬$_p$)0.0025]+⑬$_p$	0	0	0	0. 000002	0. 000006	0. 000015	0. 000030	0. 000054
⑭	7213.62×⑬	0	0	0	0. 014427	0. 043282	0. 108204	0. 216409	0. 389525
⑮	⑧+⑨+⑪+⑭	0	0. 007222	−0. 023903	−0. 319925	−0. 133053	−3. 63246	−7. 88831	−14. 7356
⑯	(150.533×⑮)+⑦	0	2662. 16	10608. 9	23538. 3	40581. 7	60220. 6	80415. 5	99028. 0
⑰	(133.919×⑤)+525.776	0	525. 924	526. 957	529. 742	535. 082	543. 648	555. 901	572. 946
⑱	−⑯/⑰	0	−5. 06187	−20. 1324	−44. 4335	−75. 8420	−110. 771	−144. 658	−173. 112
⑲	(⑱+㉘$_p$)0.0025	0	−0. 012655	−0. 062986	−0. 161415	−0. 300690	−0. 466533	−0. 638573	−0. 794425
⑳	⑲+⑳$_p$	0	−0. 012655	−0. 075641	−0. 237056	−0. 537746	−1. 00428	−1. 64285	−2. 43728
㉑	20.6673+⑳	20. 6673	20. 6546	20. 5917	20. 4302	20. 1296	19. 6630	19. 0245	18. 2300
㉒	㉑+⑲/2	20. 6673	20. 6483	20. 5602	20. 3495	19. 9793	19. 4297	18. 7052	17. 8328
㉓	㉒+⑲/2	20. 6673	20. 6420	20. 5287	20. 2688	19. 8290	19. 1964	18. 3859	17. 4355
㉔	[−0. 001398(⑦−⑯)]/32.2	0	0. 000047	−0. 000156	−0. 002093	−0. 008696	−0. 023740	−0. 051552	−0. 096297
㉕	⑱/32.2	0	−0. 157201	−0. 625230	−1. 37992	−2. 35534	−3. 44009	−4. 49248	−5. 37615
㉖	(525.776×㉘)+(715.217×㉔)/1240.99	0	−0. 066575	−0. 264983	−0. 585844	−1. 00291	−1. 47116	−1. 93306	−2. 33323

APPENDIX B

RELATIONS BETWEEN TWO-MASS SYSTEM AND REPRESENTED STRUCTURAL MODE

The sum of the masses m_L and m_S shown in figure 1 must equal the gross mass of the represented airplane in order to obtain the proper nodal acceleration. For the hypothetical limit condition in which the wing mass is concentrated at a single point in each semispan, m_L is the actual hull mass and m_S is the actual wing mass. In order to take into account the more complex nature of the structural action for a particular mode, the determination of the ratio of these masses is necessary so that the vibrational energy of the simplified and represented systems are equal for the same vibrational amplitudes of m_L and the actual hull or point of force application.

On the basis of the theory of vibrations, for which equations are included in reference 3, the vibration energy E of the two-mass system is given by the equation

$$\frac{E}{\omega^2}=\frac{1}{2}m_L\varphi_L^2+\frac{1}{2}m_S\varphi_S^2 \tag{B1}$$

where

φ_L vibrational amplitude of m_L relative to nodal point of system

φ_S vibrational amplitude of m_S relative to nodal point of system

ω natural frequency

Since for the two-mass system the node is at the center of gravity,

$$m_L\varphi_L=m_S\varphi_S \tag{B2}$$

If equation (B1) and equation (B2) are combined, and since the total mass m is equal to the sum of the masses m_S and m_L, the following equation can be obtained for the vibrational energy E of the two-mass system:

$$\frac{E}{\omega^2}=\frac{1}{2}\frac{mm_L}{m_S}\varphi_L^2 \tag{B3}$$

The vibrational energy of the represented mode is a function of the spanwise mass distribution and mode shape. On the basis that the semispan of the airplane is divided into j sections or stations. the vibrational energy of the mode can be written as follows:

$$\frac{E}{\omega^2}=\frac{1}{2}(m_1\varphi_1^2+m_2\varphi_2^2+m_3\varphi_3^2+\ldots+m_j\varphi_j^2) \tag{B4}$$

where

m_j mass of jth spanwise section; value for semispan doubled to represent the entire span

φ_j deflection of mass at jth spanwise section relative to nodal point $(h_j+x\alpha_j)$

h_j deflection of elastic axis at jth spanwise deflection relative to nodal point

x chordwise distance from elastic axis to effective mass center

α_j torsional deflection at jth spanwise station

Equality of the vibrational amplitude of the lower mass of the simplified system to the vibrational amplitude of the hull or fuselage of the flying boat or airplane relative to the nodal point of the represented mode is expressed by the equation

$$\varphi_L=\varphi_h \tag{B5}$$

where

φ_h deflection of hull or fuselage of flying boat or airplane relative to nodal point of represented mode

The requirement of equal energy of the simplified and represented systems for the condition expressed by equation (B5) gives combination of equations (B3), (B4), and (B5) to obtain the following equation for the mass ratio of the two-mass system:

$$\frac{m_S}{m_L}=\frac{m\varphi_h^2}{m_1\varphi_1^2+m_2\varphi_2^2+m_3\varphi_3^2+\ldots+m_j\varphi_j^2} \tag{B6}$$

Computation of the natural frequency of wing modes has received a great deal of attention in connection with study of wing flutter and need not be treated herein. Incidental to calculation of the natural frequency, a mode shape is attained which, together with knowledge of the mass distribution, permits use of equation (B6). In cases in which the wing has been constructed, the mode shape and natural frequency may be determined experimentally. Equation (A4) in appendix A of the present report permits computation of the spring constant which for a given mass ratio of the simplified system gives the required natural frequency.

After the accelerations of the two masses of the simplified system have been computed, equation (A3) of appendix A fixes the magnitude of the nodal acceleration. The difference between the nodal acceleration and the hull, fuselage, or float acceleration can be taken as a measure of the oscillatory acceleration. On the basis that the structure deflects in the mode used in determining the equivalent two-mass system, the acceleration at any point is given by the equation

$$n_p=n_t+n_e\frac{\varphi_j}{\varphi_h} \tag{B7}$$

The foregoing equations, with consideration of rotatory inertia and energy, may be applied to the case of a tip float attached to a flexible wing if the stiffness and mass distribution are known and if a manner of structural deflection is assumed.

REFERENCES

1. Mayo, Wilbur L.: Theoretical and Experimental Dynamic Loads for a Prismatic Float Having an Angle of Dead Rise of 22½°. NACA RB L5F15, 1945.
2. Mayo, Wilbur L.: Analysis and Modification of Theory for Impact of Seaplanes on Water. NACA Rep. 810, 1945. (Supersedes NACA TN 1008.)
3. Biot, M. A., and Bisplinghoff, R. L.: Dynamic Loads on Airplane Structures During Landing. NACA ARR 4H10, 1944.

ATI-10 901 UNCLASSIFIED (Corr. Card 1)

National Advisory Committee for Aeronautics, Washington, D. C. SOLUTIONS FOR HYDRODYNAMIC IMPACT FORCE AND RESPONSE OF A TWO-MASS SYSTEM WITH AN APPLICATION TO AN ELASTIC AIRFRAME, by Wilbur L. Mayo. TN-1398. Aug 47, 42p., tables, graphs, dwgs.

Aircraft & Flight Equipment (1)
Water-Borne Aircraft (10)

Hydrodynamic impact - Effect on Airframe

(Request copies of this report only from Originating Agency)

Delete - This document has been superseded by AD-13 505.

UNCLASSIFIED